ELSEVIER

Journal of Quantitative Spectroscopy & Radiative Transfer 103 (2007) 67–73

Journal of Quantitative Spectroscopy & Radiative Transfer

www.elsevier.com/locate/jqsrt

Photoabsorption cross section measurements of CO_2 between 106.1 and 118.7 nm at 295 and 195 K

G. Stark[a,*], K. Yoshino[b], P.L. Smith[b], K. Ito[c]

[a]*Physics Department, Wellesley College, Wellesley, MA 02481, USA*
[b]*Harvard-Smithsonian Center for Astrophysics, 60 Garden Street, Cambridge, MA 02138, USA*
[c]*Photon Factory, Institute for Materials Structure Science, High Energy Accelerator Research Organization, 1-1 Oho, Tsukuba, Ibaraki 305-0801, Japan*

Received 4 May 2006; accepted 3 July 2006

Abstract

High-resolution vacuum ultraviolet carbon dioxide photoabsorption cross sections are required for modeling airglow emissions from the Martian and Venusian atmospheres and for photochemical models of those atmospheres. We report cross section measurements on CO_2 at 295 and 195 K between 106.1 and 118.7 nm at a spectral resolution of 0.005 nm. Significant deviations from the results of previous, lower-resolution measurements are apparent, particularly in regions of sharp spectral structure. Temperature dependence in the photoabsorption cross sections is evident throughout the region, being especially pronounced at wavelengths greater than 113 nm.
© 2006 Elsevier Ltd. All rights reserved.

Keywords: Ultraviolet photoabsorption cross sections; Planetary atmospheres

1. Introduction

The photodissociation of carbon dioxide by vacuum ultraviolet (VUV) radiation is a fundamentally important photochemical process in planetary atmospheres. Photochemical models of the Earth's early atmosphere indicate significantly high concentrations of CO_2 [1,2] and identify the photodissociation of CO_2 as a primary source of prebiotic oxygen [3]. CO_2 is also the principal constituent of the atmospheres of Mars and Venus. In photochemical models of the Martian [4,5] and Venusian [6,7] upper atmospheres, the photodissociation of CO_2 by VUV solar radiation produces CO and O, with further photochemistry governing the abundances of a number of molecular species and driving the non-thermal escape of energetic atoms.

As carbon dioxide is the dominant absorber of VUV radiation in the Martian and Venusian atmospheres, its absorption spectrum determines both the depth of penetration of VUV radiation into the atmospheres and the probability of escape of VUV emissions. A recent high-resolution spectrum of the VUV airglow emissions from Mars resulted in the first detection of H_2 [8], as well as the detection of emission features from O, Ar,

*Corresponding author. Tel.: +1 781 283 3108; fax: +1 781 283 3642.
E-mail address: gstark@wellesley.edu (G. Stark).

0022-4073/$ - see front matter © 2006 Elsevier Ltd. All rights reserved.
doi:10.1016/j.jqsrt.2006.07.001

Ar^+, N, N^+, C, He, N_2 and CO [9]. Lower-resolution VUV emission spectra of Mars and Venus were reported by Feldman et al. [10]. The analyses of the new VUV observations of emission features in the Martian and Venusian atmospheres were limited by poorly and incompletely characterized CO_2 photoabsorption cross sections. In this paper we report new high-resolution photoabsorption cross sections of CO_2 that are directly applicable to analyses of atmospheric VUV airglow features and to photochemical models of planetary atmospheres.

The VUV absorption spectrum of CO_2 consists of multiple series of strong, relatively diffuse bands and regions of weak continuum absorption. Numerous optical absorption [e.g., 11–13, and references therein] and electron energy-loss [14,15] studies of CO_2 in this region have been carried out over the years. However, because of the relative diffuseness of the CO_2 features, the spectroscopic analyses have been largely limited to electronic assignments (with the exceptions of rotationally resolved studies of the 110.6 nm Rydberg state [11,13]). Theoretical studies of the absorption spectrum have addressed interactions of electronic states and spectroscopic assignments [16–20], and there has been limited theoretical work on photoabsorption cross sections and oscillator strengths [21–23].

Early VUV photoabsorption cross section measurements [24–26] suffered from insufficient instrumental resolution and inadequate attention to saturation effects (see Hudson [27] for a discussion of instrumental resolution effects). The 120–190 nm region was re-measured, at higher resolution and at multiple temperatures, by Lewis and Carver [28], Yoshino et al. [29], and Parkinson et al. [30]. With the availability of these measurements, which produced results in close agreement with one another, the CO_2 cross sections in this region are considered to be well known. However, absorption cross sections at wavelengths below 120 nm, i.e., the region of the VUV spectrum sampled by new atmospheric airglow observations [8–10], remain uncertain. Room temperature cross sections below 120 nm were measured by Nakata et al. [25] (58–167 nm) and, more recently, by Kuo et al. [31] (104–170 nm) with instrumental resolutions of about 0.2 Å, insufficient to resolve the detailed structure of the spectrum. Cross section results are presented in a figure in the work of Nakata et al. [25] and in the form of oscillator strengths of discrete features (determined from deconvolutions of the cross section measurements) in [31]. Electron energy-loss measurements have also been employed to determine discrete and continuum oscillator strengths in the VUV wavelength region. Inelastic electron scattering measurements in the 6–203 eV region were reported by Chan et al. [32] at an energy resolution of 0.048 eV, corresponding to a spectral resolution of about 6 Å, and Green et al. [33] reported absolute differential cross sections for electron impact excitation in the 108–115 nm region.

The photoabsorption cross sections presented in this paper, covering the 106.1–118.7 nm region, were measured at a resolution of 0.05 Å. This spectral resolution allows for the determination of absolute cross sections except in the wings of the 110.6 nm Rydberg band, where weak rotational structure has been previously observed [11,13]. Our measurements were carried out at 295 and at 195 K, bracketing the temperatures appropriate to the analyses of Martian VUV airglow features.

2. Experimental procedure

All measurements were carried out on the 3-m normal-incidence vacuum monochromator on the BL-20A beam line at the Photon Factory synchrotron facility at the High Energy Accelerator Research Organization in Tsukuba, Japan. A 1200 grooves mm^{-1} grating was used in the 1st order to achieve a resolution of 0.005 nm (FWHM) with entrance and exit slit widths of 20 μm. A 12-cm stainless steel absorption cell, equipped with LiF windows and a photomultiplier tube with a CsI-coated photocathode, was mounted behind the exit slit of the monochromator. The cell could be cooled to 195 K by immersion in a dry ice-ethanol slush.

Carbon dioxide was used in natural isotopic abundance ($^{12}C^{16}O_2$ 98.4%) and absorption cell pressures were monitored with 1 and 10 Torr capacitance manometers. As photoabsorption cross sections vary by approximately four orders of magnitude over the 106–119 nm spectral region, a wide range of CO_2 column densities was used. Room temperature absorption cell pressures ranged from approximately 0.01–10 Torr, corresponding to column densities ranging from 4.0×10^{15} to 4.0×10^{18} cm^{-2}. The 106–119 nm region was divided into three overlapping regions; absorption spectra in each region were recorded at four or five column densities.

Absorption spectra were scanned with a step size of 0.005 nm; a 1-s dwell time resulted in on the order of 100,000 counts for the background continuum per channel. The background continuum level was established by empty-cell scans before and after each set of absorption scans. The shape of the continuum was fit to a high-order polynomial and then combined with empty-cell counts at the beginning and end of each individual scan to determine a revised polynomial fit for that scan. A representative absorption scan, along with the continuum level established by the above procedure for that scan, is shown in Fig. 1. To minimize uncertainties associated with the determination of the background continuum level, CO_2 cross sections were independently measured at six fixed wavelengths in the 106–119 nm region—see Table 1. At each of the fixed wavelengths, output counts were measured without CO_2 in the absorption cell and then with CO_2 in the cell, alternatively every 60 s. Agreement within experimental uncertainties was found between the cross sections determined from absorption scans and those determined at the fixed wavelengths. The wavelength scale of our scans was determined by measurements of six atomic xenon absorption lines, the wavelengths of which are known to high precision [34]. For this purpose, the absorption of a mixed sample of CO_2 and Xe was recorded. A linear interpolation between Xe line positions was used to establish a final wavelength scale; we estimate that the wavelengths of the CO_2 cross sections are uncertain by 0.02 nm.

3. Results and analysis

The measured CO_2 absorption spectra were converted to photoabsorption cross sections through application of the Beer–Lambert law

$$\sigma(\lambda) = \frac{1}{N} \ln\left[\frac{I_0(\lambda)}{I(\lambda)}\right], \tag{1}$$

where $\sigma(\lambda)$ is the absorption cross section, N the column density of CO_2 molecules, $I_0(\lambda)$ the background continuum level, and $I(\lambda)$ the transmitted intensity. Because scattered light in the spectrometer and detector dark counts were determined to be negligible (by observing the residual count rates at strongly saturated absorption features), no corrections were applied to the data. Cross sections derived from scans at different column densities were compared for consistency. At the highest optical depths, saturation effects became noticeable, particularly for the sharpest absorption features; our final cross sections represent averages of scans with maximum optical depths not exceeding about 1.5.

Fig. 2(a) and (b) display the measured CO_2 cross sections at 295 and at 195 K over the wavelength range 106–119 nm. Uncertainties in the CO_2 column density and the background continuum level, as well as statistical scatter in the transmitted intensity counts all contribute to the estimated uncertainty in the cross section derived from each individual scan. The column density uncertainty arises from uncertainties in the length of the absorption cell (2 mm, or 1.5%), the temperature of the CO_2 gas (1 K, or 0.3% at 295 K and

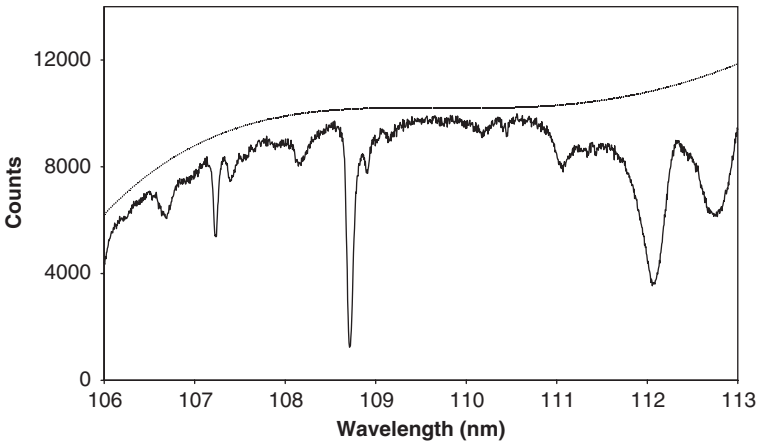

Fig. 1. Representative absorption scan of CO_2 at 295 K and background continuum level.

Table 1
A representative comparison of 295 K cross sections[a] from optical absorption measurements

Wavelength (nm)	Present results[b]	Nakata et al.[c]	Kuo et al.[d]
107.89	5.9[e]	10.9	6.0
109.77	4.4	5.9	5.0
111.44	27	34	24
112.92	95	130	80
114.2	16	20	17
115.69	5.2	5.6	5.0
107.35	95[f]	51	50
108.84	480	265	120

[a]All cross sections are in units of 10^{-18} cm^2.
[b]Uncertainties range from 5% to 10%; see text.
[c]Ref. [25].
[d]Ref. [31].
[e]The following six entries for the present work correspond to fixed-wavelength cross section measurements.
[f]The following two entries for the present work correspond to cross sections of strong, sharp features measured in scanning mode.

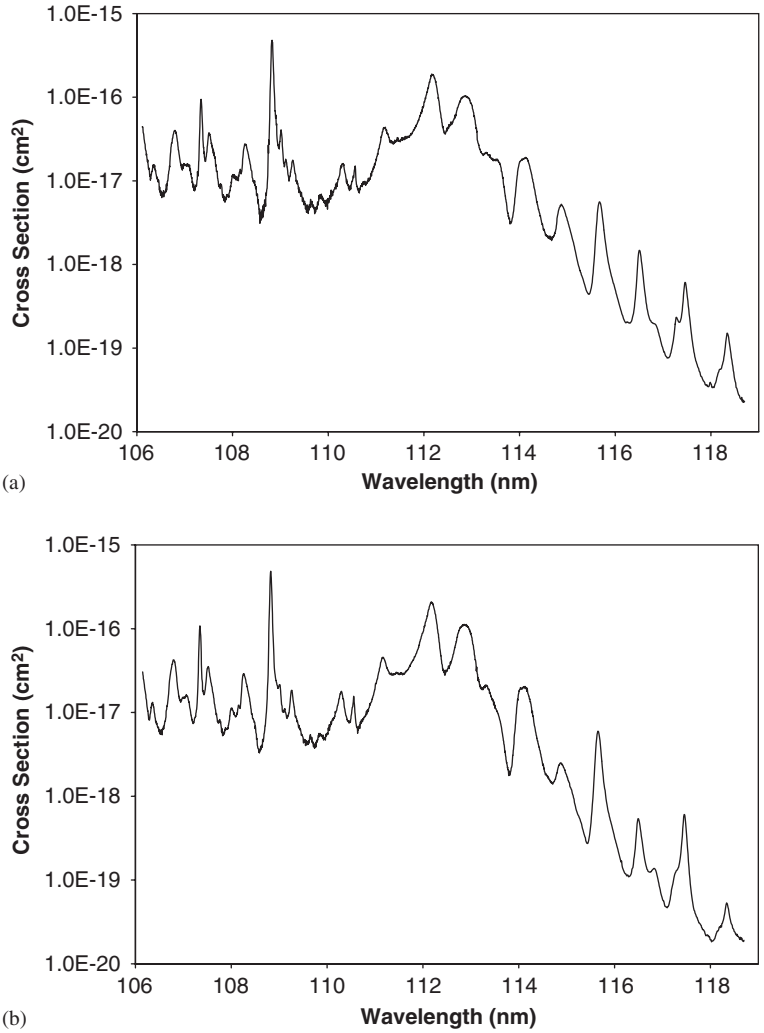

Fig. 2. (a) Photoabsorption cross section of CO_2 at 295 K; and (b) photoabsorption cross section at 195 K.

0.5% at 195 K), and the absorption cell pressure (ranging from 10% for the lowest measured pressure to less than 1% for the highest measured pressure). Our determination of the background continuum level for each absorption scan has an estimated uncertainty of 2%. The uncertainties in our final cross sections vary somewhat with wavelength; we estimate a 5% uncertainty (one standard deviation) in the cross sections in regions of peak and moderate absorption and a 10% uncertainty in regions of weakest absorption.

Temperature dependence in the photoabsorption cross section is evident throughout the 106–119 nm region. At wavelengths shortward of 112 nm, the temperature dependence is largely limited to discrete features associated with hot bands. Fig. 3 displays 295 and 195 K cross sections in the region of the strong Rydberg band identified as the $\tilde{X}\ ^1\Sigma_g^+(0,0,0) \rightarrow 3p\sigma_u\ ^1\Pi_u(0,0,0)$ transition [12]. The rapidly varying CO_2 cross sections in this region must be correctly modeled to interpret the strong Martian airglow feature associated with the carbon monoxide $E(0) \rightarrow X(0)$ transition with a band origin at 108.79 nm [9]. The effect of temperature on the cross section of the $\tilde{X}(0,1,0) \rightarrow {}^1\Pi_u(0,1,0)$ hot band at 109.02 nm is apparent, as is the temperature-dependence of the weak feature at 109.12 nm, identified by Cossart-Magos et al. [12] as a transition terminating on a $3p\,^3\Pi_u$ level. Fig. 4 shows the temperature dependence of the CO_2 cross section in the

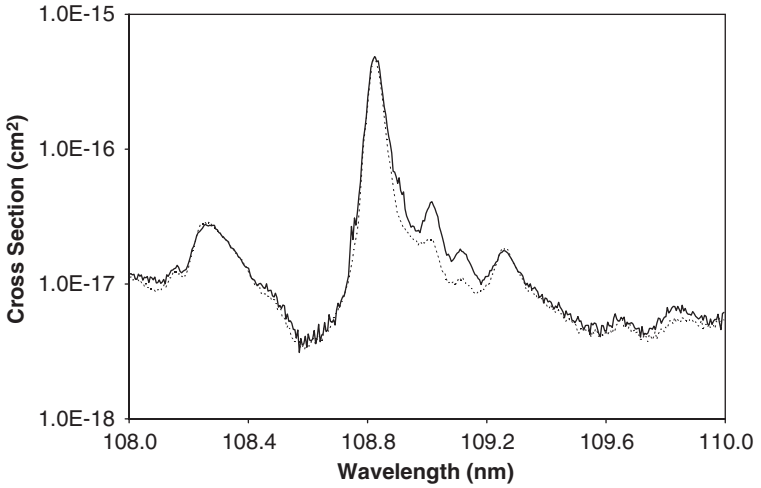

Fig. 3. A comparison of photoabsorption cross sections at 295 K (solid line) and 195 K (dashed line) in the region of the $\tilde{X}\ ^1\Sigma_g^+(0,0,0) \rightarrow 3p\sigma_u\ ^1\Pi_u(0,0,0)$ Rydberg transition. Hot bands are evident at 109.02 and 109.12 nm.

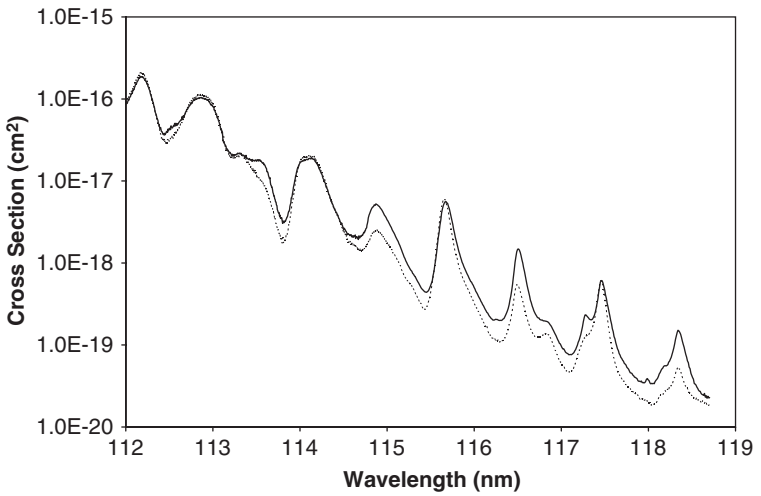

Fig. 4. A comparison of photoabsorption cross sections at 295 K (solid line) and 195 K (dashed line) in the 112–119 nm region.

112–119 nm region, where a broader pattern is evident in which the 195 K cross sections are consistently lower than the 295 K cross sections. The differences in the 295 and 195 K cross sections are quite pronounced at the longest wavelengths; for example, at the peak of the weak feature at 118.37 nm the 295 K cross section is almost a factor of three larger than the 195 K cross section. It is interesting to note that the peak cross sections of the short progression of Rathenau "double, strong" bands [35,36] appear to be temperature-independent while the peak cross sections of the Rathenau "double, weak" bands show a clear temperature dependence.

There is a small region of overlap (~1 nm in width) between the present cross section measurements at 195 K and those reported by Yoshino et al. [29] for the 118.7–175.5 nm region (using the same apparatus as in the present measurements). Within this region, the two sets of results are generally consistent to within the reported uncertainties. The two sets of 295 K measurements do not overlap. The room temperature cross section results of Nakata et al. [25] and of Kuo et al. [31] are presented in Figs. 4 and 5, and Fig. 3, respectively, of their publications. Visual comparisons with our new data reveal differences in the regions of sharpest structure, as could be anticipated from the difference in spectral resolution (0.2 Å for [25] and [31] versus 0.05 Å in the present study). Table 1 compares our 295 K cross sections measured at six fixed wavelengths with cross sections determined from the figures of Refs. [25,31]. The cross sections of Nakata et al. [25] are larger than those reported in this paper by factors ranging from ~10% to ~85%; the cross sections of Kuo et al. [31] are all within about 15% of our values. Also included in the table are cross section comparisons at the peaks of two of the strongest and sharpest features in the 106–119 nm region, at 107.35 and 18.84 nm. The effect of instrumental resolution is evident in these comparisons; the cross sections determined from the lower resolution measurements being factors of 2–3 times lower than reported here.

Numerical tabulations of the 295 and 195 K cross sections reported here can be obtained from the authors and are also available at http://cfa-www.harvard.edu/amdata/ampdata/cfamols.html. Our future work on CO_2 will extend our high-resolution measurements to the 90–106 nm region.

Acknowledgments

This work was supported by NASA grant NNG05GA03G to Wellesley College. The measurements were carried out under the approval of the Photon Factory Advisory Committee (proposal 03G151). The staff of the Photon Factory is gratefully acknowledged for their hospitality. The authors thank Paul Feldman for suggesting this measurement program and for helpful discussions.

References

[1] Kasting JF, Ackerman TP. Climatic consequences of very high carbon dioxide levels in the earth's early atmosphere. Science 1986;234:1383–5.
[2] Kasting JF. Theoretical constraints on oxygen and carbon dioxide concentrations in the Precambrian atmosphere. Precambrian Res 1987;23:205–29.
[3] Kasting JF, Liu SC, Donahue TM. Oxygen levels in the prebiological atmosphere. J Geophys Res 1979;84:3097–107.
[4] Nair H, Allen M, Anbar AD, Yung YL. A photochemical model of the Martian atmosphere. Icarus 1994;111:124–50.
[5] Fox JL, Bakalian FM. Photochemical escape of atomic carbon from Mars. J Geophys Res 2001;106:28,785–95.
[6] Fox JL, Sung KY. Solar activity variation of the Venus thermosphere/ionosphere. J Geophys Res 2001;106:21305–35.
[7] Fox JL, Paxton LJ. C and C^+ in the Venusian thermosphere/ionosphere. J Geophys Res 2005;110:A01311.
[8] Krasnopolsky VA, Feldman PD. Detection of molecular hydrogen in the atmosphere off Mars. Science 2001;294:1914–7.
[9] Krasnopolsky VA, Feldman PD. Far ultraviolet spectrum of Mars. Icarus 2002;160:86–94.
[10] Feldman PD, Burgh EB, Durrance ST, Davidsen AF. Far-ultraviolet spectroscopy of Venus and Mars at 4 Å resolution with the Hopkins Ultraviolet Telescope on Astro-2. Astrophys J 2000;538:395–400.
[11] Cossart-Magos C, Leach S, Eidelsberg M, Launay F, Rostas F. Rationally resolved Rydberg absorption of CO_2 at 1106 Å. J Chem Soc 1982;78:1477–87.
[12] Cossart-Magos C, Jungen M, Launay F. High resolution absorption spectrum of CO_2 between 10 and 14 eV. Mol Phys 1987;61:1077–117.
[13] Yang XF, Lemaire JL, Rostas F, Rostas J. VUV laser-absorption study at 110.6 nm of the rotationally structured … $1\pi_g^3 3p\pi_u\,{}^3\Sigma_u^-$ Rydberg state of CO_2. Chem Phys 1992;164:115–22.
[14] McDiarmid R, Doering JP. Electronic excited states of CO_2: an electron impact investigation. J Chem Phys 1984;80:648–56.
[15] Hubin-Franskin M-J, Delwiche J, Leclerc B, Roy D. Electronic excitation of carbon dioxide in the 10.5–18 eV range studied by inelastic electron scattering spectroscopy. J Phys B 1988;21:3211–29.

[16] Werner H-J, Spielfiedel A, Feautrier N, Chambaud G, Rosmus P. On the Rathenau bands in the absorption spectrum of CO_2. Chem Phys Lett 1990;175:203–8.
[17] Winter NW, Bender CF, Goddard WA. Theoretical assignments of low-lying electronic states in carbon dioxide. Chem Phys Lett 1973;20:489–92.
[18] Spielfiedel A, Feautrier N, Chambaud G, Rosmus P, Werner HJ. Interactions of Rydberg and valence states in CO_2. Chem Phys Lett 1991;183:16–20.
[19] Spielfiedel A, Feautrier N, Cossart-Magos C, Chambaud G, Rosmus P, Werner HJ, et al. Bent valence excited-states of CO_2. J Chem Phys 1992;97:8382–8.
[20] Spielfiedel A, Feautrier N, Chambaud G, Rosmus P, Werner HJ. The 1st dipole-allowed electronic transition of CO_2. Chem Phys Lett 1993;216:162–6.
[21] Padial N, Csanak G, McKoy BV, Langhoff PW. Photoexcitation and ionization in carbon dioxide: theoretical studies in the separated-channel static-exchange approximation. Phys Rev A 1981;23:218–35.
[22] Buenker RJ, Honigmann M, Liebermann H-P. Theoretical study of the electronic structure of carbon dioxide: bending potential curves and generalized oscillator strengths. J Chem Phys 2000;113:1046–54.
[23] Olallo E, Martín I. Theoretical study of the valence and K-shell spectra of atmospherically relevant CO_2. Int J Quant Chem 2004;99:502–10.
[24] Inn ECY, Watanabe K, Zelikoff M. Absorption coefficients of gases in the vacuum ultraviolet. Part III, CO_2. J Chem Phys 1953; 21:1648–50.
[25] Nakata RS, Watanabe K, Matsunaga FM. Absorption and photoionization coefficients of CO_2 in the region 580–1670 Å. Sci Light 1965;14:54–71.
[26] Ogawa M. Absorption cross sections of O_2 and CO_2 continua in Schumann and far-uv regions. J Chem Phys 1971;54:2550–6.
[27] Hudson RD. Critical review of ultraviolet photoabsorption cross sections for molecules of astrophysical and aeronomic interest. Rev Geophys 1971;9:305–406.
[28] Lewis BR, Carver JH. Temperature dependence of the carbon dioxide photoabsorption cross section between 1200 and 1970 Å. J Quant Spectrosc Radiat Trans 1983;30:297–309.
[29] Yoshino K, Esmond JR, Sun Y, Parkinson WH, Ito K, Matsui T. Absorption cross section measurements of carbon dioxide in the wavelength region 118.7–175.5 nm and the temperature dependence. J Quant Spectrosc Radiat Transfer 1996;55:53–60.
[30] Parkinson WH, Rufus J, Yoshino K. Absolute absorption cross section measurements of CO_2 in the wavelength region 163–200 nm and the temperature dependence. Chem Phys 2003;290:251–6.
[31] Kuo CT, Chen YM, Wang SY, Li SC, Nee JB. The photoabsorption spectrum of CO_2 at 104–170 nm. Chin J Phys 2004;42:65–73.
[32] Chan WF, Cooper G, Brion CE. The electronic spectrum of carbon dioxide. Discrete and continuum photoabsorption oscillator strengths (6–203 eV). Chem Phys 1993;178:401–13.
[33] Green MA, Teubner PJO, Campbell L, Brunger MJ, Hoshino M, Ishikawa T, et al. Absolute differential cross sections for electron impact excitation of the 10.8–11.5 eV energy-loss states of CO_2. J Phys B 2002;35:567–87.
[34] Yoshino K, Freeman DE. Absorption spectrum of xenon in the vacuum-ultraviolet region. J Opt Soc Am B 1985;2:1268–74.
[35] Rathenau G, Z Physik 1934;87:32.
[36] Tanaka Y, Jursa AS, LeBlanc FJ. Higher ionization potentials of linear triatomic molecules: I. CO_2. J Chem Phys 1960;32:1199–205.